JOURNAL OF SPACECRAFT AND ROCKETS
Vol. 42, No. 6, November–December 2005

Effects of Space Environment Factors on Optical Materials

Hai Liu,* Geng Hongbin,* Shiyu He,* and Dezhuang Yang*
Harbin Institute of Technology, 150001 Heilongjiang, People's Republic of China
V. V. Abraimov
Kharkov National University, 60164, Kharkov, Ukraine
and
Huaiyi Wang
508 Institute of Space Technology Academy of China, 100076 Beijing, People's Republic of China

The effects of protons and electrons, as well as thermocycling, on surface morphology and optical properties of beryllium-base reflector and JGS3 optical quartz glass were studied. The energy of protons and electrons was in the range of 60–180 keV, and the thermocycling temperature interval $T = 80$–403 K. The results showed that after the radiations for a critical fluence of $\Phi = 6 \times 10^{15}/\text{cm}^2$ the surface morphology of beryllium-base reflector was damaged severely. The radiations tended to induce spotted pits on the reflector surface with thicker SiO_2 layer and bubbles on that with thinner SiO_2 layer. The surface damage was aggravated by thermocycling following the radiations and affected by grounding conditions. The JGS3 glass was colored evidently after the fluence reached $\Phi = 10^{15}/\text{cm}^2$ for the protons and $\Phi = 5 \times 10^{14}/\text{cm}^2$ for the electrons. The protons mainly induced the absorption bands at 209 and 220–240 nm and the electrons the bands at 203 and 215 nm. Under the fluence less than $\Phi = 2 \times 10^{16}/\text{cm}^2$, the absorptions increased with fluence monotonically. The E'-type centers were responsible for the absorptions at 203–215 and 220–240 nm.

Introduction

As is known, spacecraft flying in orbits from 300 to 36,000 km are subjected to these space environment factors: vacuum ($P = 10^{-4}$–10^{-12} Pa), solar electromagnetic rays, protons and electrons with energy $E = 0.03$–10 MeV in Van Allen radiation belts, ionosphere and magnetosphere plasma, atomic oxygen, and wide-range thermocycling.[1–4] These environmental factors would result in degradation of materials on spacecrafts. The optical systems as a payload on spacecrafts are responsible for weather and resource monitoring, satellite positioning, and astronomic observations. After long-time effects of space environment, the sensitivity of optical systems could be decreased and even be out of service.[5–7]

In previous work, most studies about radiation effects of charged particles on spacecrafts focused on the particles with energy greater than 1 MeV. Because the flux of particles decreases with increasing energy in the Van Allen radiation belts, the particles with energy less than 200 keV have large fluxes up to $10^8/\text{cm}^2 \cdot \text{s}$. It is known that the lower the particle energy, the relatively shorter the penetration depth of particles into materials. Under the radiation of particles with energy less than 200 keV, the energy absorbed by space materials is mainly concentrated in the surface layer. Reasonably, the effects of particles with such lower energy on optical materials should be important and not be neglected, especially for spacecraft with long lifetimes. The reflective property of reflectors reduces after a certain radiation fluence of protons and electrons. It was found that the proton radiation can cause a special blistering phenomenon.[8] On glass materials, a main influence of the radiation is to decrease the transmittance in a given wavelength range and to colorate the materials. The coloration results from the particular color centers inside the glass. In the quartz glass, the E'-type centers led to some intrinsic absorption bands.[9–11] In this work, the changes in surface morphology and optical property of beryllium-base reflector and optical quartz glass were studied under radiations of protons and electrons with energy 60–180 keV and thermocycling in the temperature range from 80 to 403 K.

Received 9 September 2002; revision received 1 January 2003; accepted for publication 8 August 2003.

*Space Materials and Environment Engineering Laboratory, Harbin.

Experimental

The ground simulation test was carried out using a facility that can simulate the space environment factors: vacuum (10^{-5} Pa), cold black background (77 K), radiations of protons and electrons with energy less than 200 keV, solar electromagnetic rays ($\lambda = 5$–2500 nm), and thermocycling from 77 to 403 K (Refs. 12 and 13).

The specimens were divided into two groups, including the plane beryllium-base reflector and the JGS3 optical quartz glass ones. As shown in Fig. 1, the reflectors had a plane multilayer structure, in which the 0.5-mm-thick glass and 0.1-mm-thick copper layers were adhered to the beryllium substrate with diameter of 60 mm and thickness of 10 mm, respectively; the 1000-nm-thick silver layer was vapor deposited on the glass or copper layer in vaccum; the 100- and 50-nm-thick SiO_2 protective layers were plasma splayed on to the silver layer, respectively. Before the radiations, the reflectivity of the beryllium-base reflector was approximately 90% in the wavelength range of 0.25–0.3 μm. During the radiations, the reflectors were grounded directly through a platform and a capacitor with 20-kV breakdown potential, respectively. The former grounding mode is often adopted in the radiation tests, and the latter is closer to the situation on spacecrafts in orbit.

The JGS3 glass is a Chinese trade brand optical quartz one, which was produced by melting high-quality pure natural rock or cultured crystals in electric furnaces in vacuum using a graphite crucible. The glass is almost free of OH and contains less than 50 ppm metallic impurities. The original average transmittance was about 92% in the wavelength range from 0.26 to 3.5 μm. The JGS3 glass samples had the geometry of $\phi 20 \times 2$ and $\phi 10 \times 2$ mm.

The experimental parameters for radiations of protons and electrons were chosen as the energy 60–200 keV; the beam density $J = 0.1\ \mu\text{A/cm}^2$; and the radiation fluence $\Phi = 10^{14}$–10^{17} part/cm^2. The thermocycling ($T = 80$–403 K) was performed after radiations, in which the cooling was realized by thermal conduction and the heating by infrared radiation.

Results and Discussion

Investigation on Beryllium-Base Reflector

Either proton or electron radiation, after reaching a given fluence, would cause degradation of reflectivity and imaging quality.

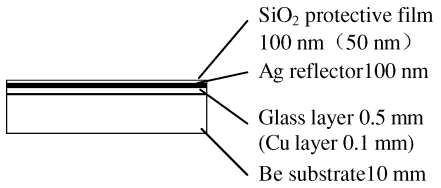

Fig. 1 Configuration and dimension of the tested reflector.

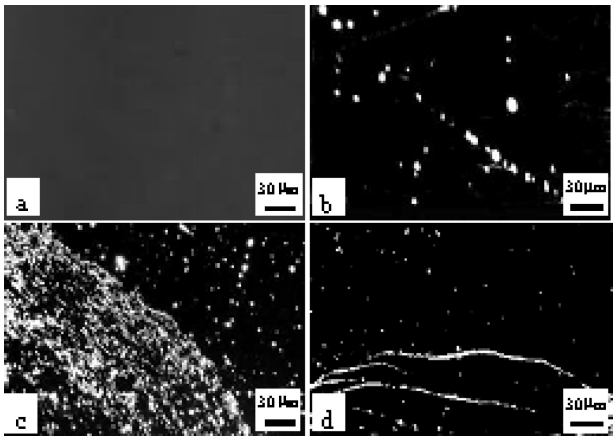

Fig. 2 Surface morphologies of the reflector with 100-nm-thick SiO_2 layer before and after radiation of protons and electrons with energy $E_p = E_e = 160$ keV and fluence $\Phi_p = \Phi_e = 5 \times 10^{16}$ part/cm^2: a) before radiation; b) radiated, grounding through a platform; and c) and d) radiated, grounding through a capacitor.

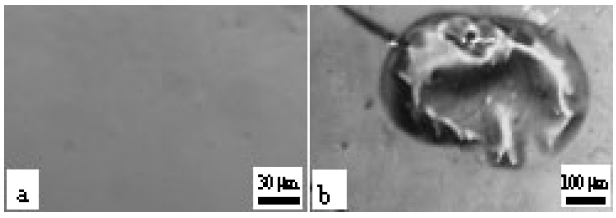

Fig. 3 Surface morphologies of the reflector with 50-nm-thick SiO_2 layer a) before and b) after radiation of protons with energy $E_p = 130$ keV and fluence $\Phi_p = 10^{16}$ part/cm^2.

In particular, under the proton radiation the surface morphology of the beryllium-base reflector might be damaged. The damage was associated with reflector configuration and grounding mode. Figure 2 presents surface morphologies of the reflector with the 100-nm-thick SiO_2 layer after radiations. In the case of the first grounding mode, spotted pits, which were sized in the range of 1–10 μm, formed and were dispersed on the specimen surface (Fig. 2b). There exists a critical radiation fluence $\Phi = 6 \times 10^{15}$/cm^2 to cause this kind of damage. For the second grounding case, not only the preceding dispersed pits but densely distributed defect bands appear on the radiated surface. The bands seem as streams to flow regularly from the specimen center to its edges (Fig. 2c). In some regions near the reflector edges, the SiO_2 reflective layer was exfoliated from the substrate (Fig. 2d).

After the proton radiation, the spotted pits on the reflector with 100-nm-thick SiO_2 layer are crateriform (Fig. 2b), whereas on that with the SiO_2 layer thickness of 50 nm, blistering occurred, forming bubbles with an irregular shape and average size greater than 100 μm in a small amount (Fig. 3b). After the proton radiation followed by thermocycling in the range of $T = 80 \sim 403$ K, the reflector surface was damaged much more severely. On some areas, the reflective Ag layer peeled off completely, and an extensive bulging occurred, as shown in Fig. 4.

From the preceding results, it is reasonable to assume that under proton radiation the formation of spotted pits and bubbles on the

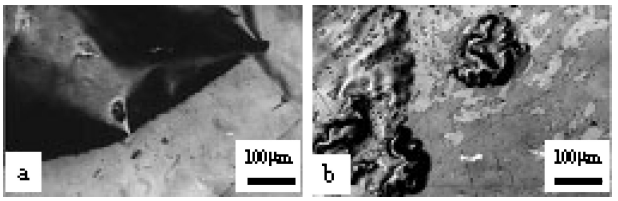

Fig. 4 Surface morphologies of the reflector with 50-nm-thick SiO_2 layer after proton radiation and eight times thermocycling between 80 and 403 K: a) peeling of the Ag layer and b) bulging of the Ag layer.

reflector surface might result from the same mechanism, namely, aggregation and expansion of hydrogen. Generally, the optical surface layers have a thickness less than 0.1 μ, which is less than the penetrating depth of the protons with energy less than 200 keV into materials (about 1–2 μ). When many of the protons were implanted into a reflector, they would aggregate to form hydrogen gas and microbubbles under the surface layers. With increasing proton fluence, the microbubbles keep growing up to destroy the layers. The different damages of surface morphology were associated with the thickness of SiO_2 protective layer. A fairly thicker surface protective layer on the reflector is in favor of restraining plastic deformation of the Ag reflective layer; thus, local blisters were formed under the pressure of hydrogen. On the other case, the SiO_2 protective layer is so thin that the Ag layer can deform freely to form fairly large bubbles.

On the basis of radiation-induced bubbling theory presented by Guseva and Martinenko,[14] one can estimate roughly a critical radiation fluence for macrobubble formation:

$$\Phi = (\sigma_F / H) \cdot \sqrt{\delta R^2(E)} \tag{1}$$

where σ_F is the ultimate strength of materials, H the implanting energy of hydrogen atoms, and δR^2 the mean-square deviation of proton penetrating depth. Therefore, from the experimental parameters for this study the theoretic critical fluence could be calculated as about $\Phi = 4 \times 10^{15}$/cm^2. It conformed well with the observed critical value.

Under the grounding mode through a capacitor, severe damage of the reflector resulted not only from the bubbling mechanism but mainly from an electrostatic effect. Charged particle radiation could create surface charging of dielectric materials, and the implantation of heterogeneous charges into the materials might even cause a body charging. No matter what kind of charging mode, charges accumulated to some degree would create discharging. The very high instantaneous discharging current, followed by a large amount of heat, leads to a severe damage of the reflector surface through the discharging path.

Owing to different expansion coefficients between the layers on the reflector, thermocycling causes an inconsistent deformation between the surface layers and the interlayer stresses. Once the interlayer stress is high enough, it would destroy the surface layers. A great deal of hydrogen gas within the reflector, accumulated during proton radiation, tends to diffuse to the surface and boundaries and finally cause the surface layers to be bulged or peeled over large areas.

Investigation on Quartz Glass

Figure 5 shows the changes in spectral transmittance of JGS3 optical quartz glass before and after radiations of protons and electrons with different energy and fluence. It indicates that after the proton radiation fluence reached 10^{15}/cm^2, the spectral performance of the JGS3 glass degraded distinctly. With increasing the fluence, the change in transmittance firstly occurred in the near-ultraviolet region and gradually spread to longer wavelengths. But little influence was observed in the infrared region. The transmittance monotonously decreased in the near-ultraviolet to visible regions with increasing the fluence to 2×10^{16}/cm^2. The change in spectral transmittance of the JGS3 glass after electron radiation was similar to that caused by the protons. However, the critical fluence of electrons was

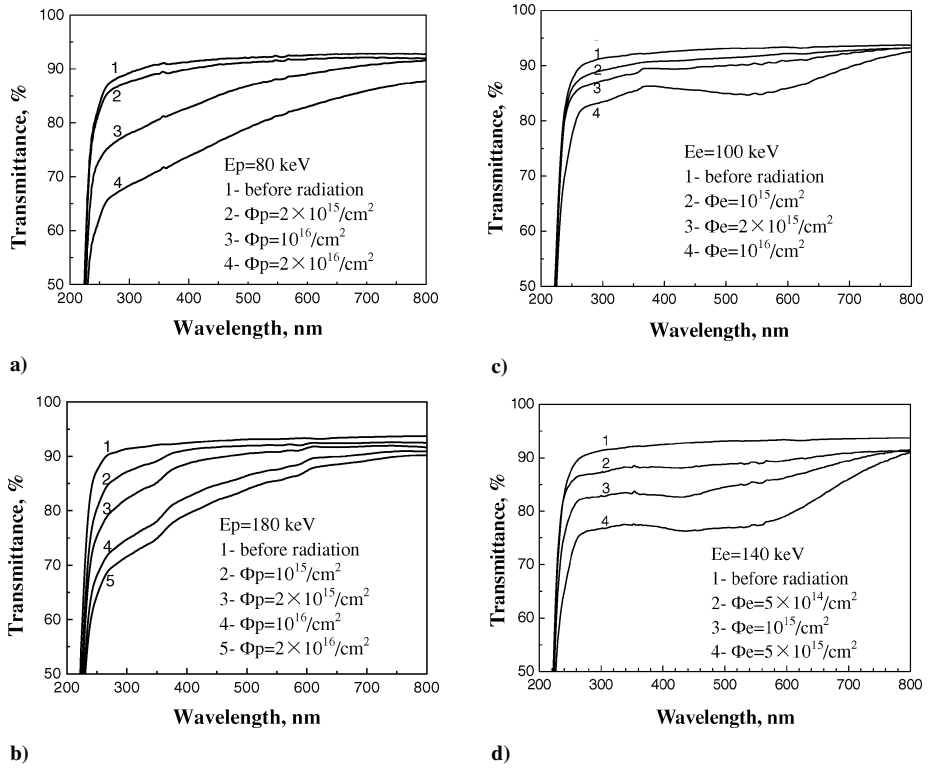

Fig. 5 Spectral transmittance of JGS3 optical quartz glass before and after radiation of protons and electrons with various energy and fluences: a) proton radiation, $E = 80$ keV; b) proton radiation, $E = 180$ keV; c) electron radiation, $E = 100$ keV; and d) electron radiation, $E = 140$ keV.

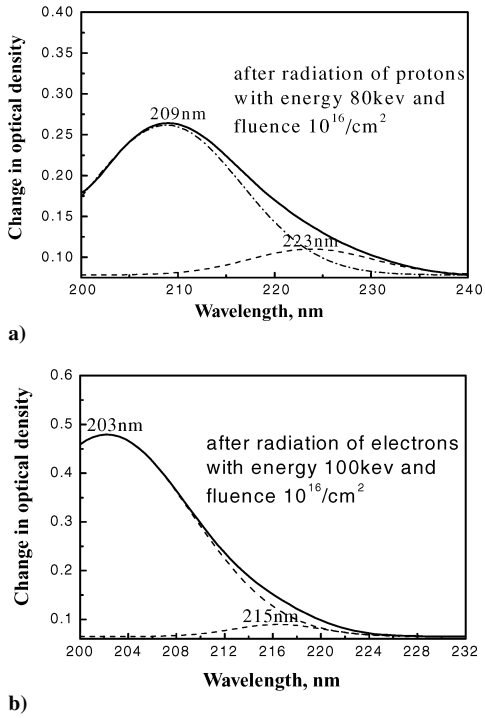

Fig. 6 Absorption spectrum of JGS3 optical quartz glass after radiations of a) protons with energy $E_p = 80$ keV and b) electrons with energy $E_e = 100$ keV.

approximately $5 \times 10^{14}/\text{cm}^2$ for obvious transmittance change, and a greater decrease in spectral transmittance appeared at the wavelengths of 200–800 nm than that caused by protons with the same energy and fluence.

Figure 6 shows the absorption spectra in near-ultraviolet region of the JGS3 glass after radiations of protons and electrons. Figure 6a indicates that the proton radiation primarily resulted in absorption in the vicinity of 209 nm. Another absorption peak appeared in the wavelength region of 220–240 nm. With increasing the proton fluence, both of the absorption peaks increased and moved to longer wavelengths. The ultraviolet absorption spectrum after the electron radiation is shown in Fig. 6b, in which the main absorption peaks are located at approximately 203 and 215 nm, respectively. In addition, under higher radiation fluences the radiations of protons and electrons could induce weaker absorption peaks, such as the peaks at 300 and 450 nm for the protons, and those at 300, 400–420, and 530–550 nm for the electrons. In general, under the radiation fluences chosen in this study the absorption peaks increased with the fluence monotonically, but the absorption peak at 550 nm caused by electron radiation began to decrease after the fluences more than $10^{16}/\text{cm}^2$.

It was believed that all of the absorption peaks at 203, 209, and 215 nm originated from the E'-type centers.[15,16] The typical E'-type center is an E_1' center, an oxygen vacancy having an unpaired electron localized in the sp^3 hybrid orbit extending into the vacancy from the adjacent silicon ion on the short-bond side of the vacancy. Such oxygen vacancies could be generated during the glass manufacturing and radiations. The E_1' center can be changed into the E' center variants by disturbing with impurities such as H. Under the proton radiation, many bonds in the quartz glass would be broken, and the hydrogen easily reacts with the broken bonds. For instance, the possible reactions could be as follows:

$$\equiv \text{Si} + \text{H} \xrightarrow{p} \text{Si} - \text{H} \tag{2}$$

$$\equiv \text{Si} - \text{O} + \text{H} \xrightarrow{p} \equiv \text{Si} - \text{OH} \tag{3}$$

After the reactions, the structure of E' centers would be changed, forming the E' center variants, such as E_2' and E_4' centers,[17] which were responsible for the absorption bands at 220–240 nm.

Because the E' center is a kind of paramagnetic defect, the preceding speculation could be confirmed by the electron spin resonance analysis (ESR). Figure 7 showed the ESR spectra for the JGS3 glass after an radiations of protons and electrons. In both of the cases, strong signals of resonance were obtained, indicating that a lot of paramagnetic defects were induced in the quartz glass. The g values were equal to 2.0011 and 2.0017 after the proton and electron

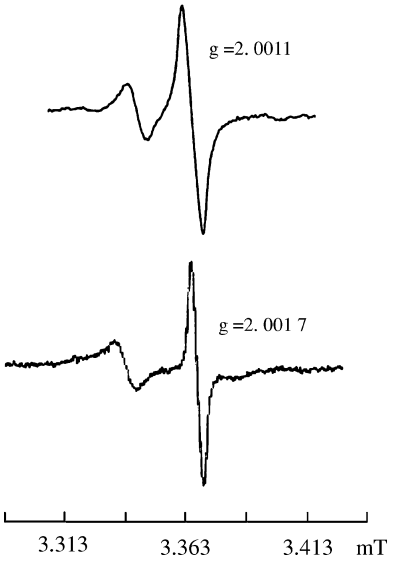

Fig. 7 Electron spin resonance spectra of JGS3 optical glass after radiations of a) protons with energy $E_p = 140$ keV and fluence $\Phi_p = 10^{16}$ part/cm^2 and b) electrons with energy $E_p = 100$ keV and fluence $\Phi_e = 5 \times 10^{15}$ part/cm^2.

radiation, respectively. Both of the values are less than the g value 2.0023 for free electrons. The experimental results conformed well to Refs. 18–20, which prove the formation of E' centers in JGS3 optical quartz glass as a result of the radiations. The absorption bands at the wavelengths of 300, 400–420, 450, and 530–550 nm in the JGS3 glass might be related to the impurities of Al and Na (Refs. 11, 16, 21, and 22).

Conclusions

The surface morphology of beryllium-base reflector could be damaged severely after the radiations of protons and electrons for a critical fluence of $\Phi = 6 \times 10^{15}/\text{cm}^2$. The radiations tended to induce spotted pits on the reflector surface with thicker SiO_2 protective layer, whereas bubbles formed on that with a thinner SiO_2 layer. The surface damage would be further enhanced by thermocycling following the radiations and affected by grounding conditions.

In the JGS_3 optical quartz glass, the protons mainly induced the formation of absorption peaks at 209 and 220–240 nm, and the electrons resulted in the ones at 203 and 215 nm, respectively. Under the fluence less than $\Phi = 2 \times 10^{16}/\text{cm}^2$, the absorption peaks increased with the fluence monotonically.

The absorption bands appearing in the ultraviolet region can be related to the E' centers. Under the radiation of protons, the hydrogen ions might join in bonding reactions, leading to the transitions from [≡Si–] and [≡Si–O] to [≡Si–H] and [≡Si–OH], respectively.

References

[1]Akishin, A. I., and Teplov, I. B., "Simulation of Space Radiation Effects on Materials," *Physics and Chemics in the Material Process*, No. 3, 1992, pp. 47–57.

[2]Garrett, H. B., "Space Radiation Models," AIAA Paper 94-0590, Jan. 1994.

[3]William, A., "The Space Radiation Environment: An Overview for Mir and ISS Missions," AIAA Paper 96-0928, Jan. 1996.

[4]Richard, D. L., "Spacecraft System Failures and Anomalies Attributed to the Natural Space Environment," AIAA Paper 95-3564, Sept. 1995.

[5]Nicoletta, C. A., Eubanks, A. G., "Effect of Simulated Space Radiation on Selected Optical Materials," NASA TN-D-6758, May 1972.

[6]Marshall, G. C., "Evaluation of the Effects of Solar Radiation on Glasses," NASA CR-161907, July 1979.

[7]Becher, Jacob, and Fowler, Walter, "The Simulated Space Proton Environment for Radiation Effects on Space Telescope Imaging Spectrograph," NASA CR-190618, 1992.

[8]Abraimov, V. V., Lura, F., Bone, L., Velizhko, N. I., Markus, A. M., Agashkova, N. N., and Mirzoeva, L. A., "Investigation of Blistering and Flaking Phenomena in Materials of Space Optics Under the Space Environment Factors," *Space Science and Technology*, Vol. 1, Nos. 2–6, 1995, pp. 39–54.

[9]Allen, J. L., Seifert, N., Yao, Y., Albridge, R. G., Barnes, A. V., and Tolk, N. H., "Point Defect Formation in Optical Materials Exposed to the Space Environment," NASA N95-27646, 1995, pp. 1131, 1132.

[10]Gulamova, R. R., Gasanov, E. M., and Alimov, R., "Proton-Induced Changes of Optical Properties and Defect Formation in Quartz Glasses," *Nuclear Instruments and Methods in Physics Research B*, Vol. 127/128, 1997, pp. 497–502.

[11]Marshall, C. D., Speth, J. A., and Payne, S. A., "Induced Optical Absorption in Gamma, Neutron and Ultraviolet Irradiated Quartz Glass and Silica," *Journal of Non-Crystalline Solids*, Vol. 212, 1997, pp. 59–73.

[12]Abraimov, V. V., Yang, Shiqin, He, Shiyu, Yang, Dezhuang, Kolybaev, L. K., and Verhovtseva, E. T., "Complex Simulation of the Effect of Eight Space Environment Factors on Space Vehicle Materials," *The Fifth Sino-Russian-Ukrainian Symposium on Space Science and Technology Held Jointly with the First International Forum on Astronautics and Aeronautics Symposium Proceedings*, Harbin Inst. of Technology, Harbin, PRC, 2000, pp. 706–713.

[13]Abraimov, V. V., Eremenko, V. V., Verhovtseva, E. T., Kolybaev, L. K., Zaika, A. S., Nekludov, I. M., Bors, B. V., Tolstolutskaja, G. D., He, Shiyu, Yang, Dezhuang, and Liu, Hai, "Complex Simulator of Space Environment Factors," *Journal of Kharkiv National University*, Physical Series "Nuclei, Particles, Fields," Vol. 541, No. 4–16, 2001, pp. 28–34.

[14]Guseva, M. J., and Martinenko, Y. V., "Radiation Blistering," *Progress of Physics Science*, Vol. 135, No. 4, 1981, pp. 671–691.

[15]Christopher, D. M., Joel, A. S., and Stephen, A. P., "Induced Optical Absorption in Gamma, Neutron and Ultraviolet Irradiated Fused Quartz and Silica," *Journal of Non-Crystalline Solids*, Vol. 212, 1997, pp. 59–73.

[16]Gritsyna, V. T., Bazilevskaya, T. A., Voitsenya, V. S., Orlinski, D. V., and Tarabrin, Yu. A., "Accumulation of Stable Optical Centers in Silica Glasses Under Pulse Beam Irradiation," *Journal of Nuclear Materials*, Vol. 233/237, 1996, pp. 1310–1317.

[17]Robert, A. W., "The Many Varieties of E′ Centers: a Review," *Journal of Non-Crystalline Solids*, Vol. 179, 1994, pp. 59–73.

[18]Griscom, D. L., "E′ Center in Glassy SiO_2: ^{17}O, ^{1}H, and 'Very Weak' ^{29}Si Superhyperfine Structure," *Physical Review B*, Vol. 22, No. 9, 1980, pp. 4192–4202.

[19]Griscom, D. L., "Electron Spin Resonance in Glasses," *Journal of Non-Crystalline Solids*, Vol. 40, 1980, pp. 241–245.

[20]Hosono, Hideo, Kawazoe, Hiroshi, Oyoshi, Keiji, and Tanaka, Shuhei, "Paramagnetic Resonance of E'-type Centers in Si-Implanted Amorphous SiO_2. Si^{29} Hyperfine Structure and Characteristics of Zeeman Resonances," *Journal of Non-Crystalline Solids*, Vol. 179, 1994, pp. 39–50.

[21]Gulamova, R. R., Gasanov, E. M., and Alimov, R., "Proton-Induced Changes of Optical Properties and Defect Formation in Quartz Glasses," *Nuclear Instruments and Methods in Physics Research B*, Vol. 127/128, 1997, pp. 497–502.

[22]Hattori, M., Nishihara, Y., Ohki, Y., Fujimaki, M., Souno, T., Nishikawa, H., Yamaguchi, T., Watanabe, E., Oikawa, M., Kamiya, T., and Arakawa, K., "Characterization of Ion-Implanted Silica Glass by Vacuum Ultraviolet Absorption Spectroscopy," *Nuclear Instruments and Methods in Physics Research B*, Vol. 191, 2002, pp. 362–365.

D. Edwards
Associate Editor